The design of a low-cost directional warning sound system for electric vehicles

N. Kournoutos [1], **J. Cheer** [1], **S.J. Elliott** [1]
[1] Institute of Sound and Vibration Research, University of Southampton,
University Rd, Southampton SO17 1BJ, UK
e-mail: **N.Kournoutos@soton.ac.uk**

Abstract
Electric vehicle warning sounds are now required by law in many countries due to safety concerns, but this additional noise source may increase unwanted noise pollution. Therefore, the design of an electric vehicle warning sound system that can produce a directional sound field has been investigated. This paper introduces two design suggestions for a system with comparable performance to the conventional loudspeaker array, but at a significantly lower manufacturing and maintenance cost, suitable for wider commercial adoption. The first method utilises a single loudspeaker attached to a length of perforated piping which acts as a directional acoustic radiator, which is analogous to the shotgun microphone. The second approach replaces the standard loudspeaker array with inertial actuators mounted to a vehicle body panel and these are driven to radiate a controlled directional sound field. A simulation based comparison between the suggested configurations and a conventional loudspeaker array of equivalent physical dimensions is presented.

1 Introduction

Within the past couple of decades, Electric Vehicles (EVs) and Hybrid-Electric Vehicles (HEVs) have increased their share of the passenger vehicle market, and given the desire and support of public and authorities alike for ecologically friendlier means of transportation, it is reasonable to assume that this presence is only going to grow stronger in the future. A wider integration of EVs in public and private transport should result in better living conditions for urban areas, with reduced air pollution due to lower carbon dioxide emissions, and reduced noise pollution, due to the quiet operation of electric motors [1].

Focussing on the subject of noise generated by vehicles, it has been studied and established that indeed EVs produce significantly less engine noise than Internal Combustion Engine (ICE) equipped vehicles. However, it is factors such as aerodynamics and the interaction of tyres with the road that dominate as noise sources for higher speeds, at which both types of vehicle produce similar noise levels [2]. Still, research results point out that for speeds below the 30 km/h limit, EVs are consistently quieter compared to typical ICEs [3].

A point of concern regarding this quiet operation of EVs is the lack of detectability it may provide for pedestrians, cyclists and other vulnerable road users. Researchers and institutions have investigated the extent to which this lack of audible cues poses a safety issue and whether it necessitates the use of external warning sounds for EVs. Though results do not unanimously reach a verdict [4], [5], and opposition to the adoption of warning sounds has been expressed [6], legislation for the mandatory use thereof has been coming into effect across different countries [7], [8]. For the purpose of rendering vehicles audibly detectable while avoiding excessive unwanted noise, surveys have been conducted to determine the characteristics of an effective warning sound. The guidelines for Acoustic Vehicle Alerting Systems (AVAS) first initiated by

the European Commission are being adopted globally and constitute a standard manufacturers of EVs are required to meet [9].

Apart from refining the content of the warning sound itself, an approach to ensure detectability while minimising the vehicle's overall contribution to noise is to generate a directional sound field. In-depth research on a directional warning sound system has been performed in the past through the European Commission project eVADER (electric Vehicle Alert for Detection and Emergency Response), which included investigation of methods to direct the sound field at specific targets identified as vulnerable road users [10], [11], [12]. The suggested solution uses an array of loudspeakers installed at the front bumper of the vehicle, which can achieve a high degree of selective beamforming. However, such a configuration requires a high cost of manufacture and maintenance due to its components, especially if intended for implementation in affordable passenger vehicles.

The aim of this paper is to investigate methods that are capable of producing directional sound fields, and that are suitable for integration as warning sound systems for EVs, while maintaining a lower cost than conventional loudspeaker arrays. Two approaches to designing such a system are investigated. The first concept is a low cost acoustic radiator consisting of a single loudspeaker attached to a perforated pipe, which generates the directivity of an end-fire array that would otherwise require multiple sound sources. The second approach utilises an array of structural actuators, lower in cost and potentially more robust than loudspeaker drivers, which force the vibration of a panel–possibly belonging to the body of the vehicle. By controlling this vibration, the system can be tuned to achieve a directional sound field with selective beamforming capabilities.

Section 2 introduces the principles of operation and the mathematical models used to simulate a conventional multiple loudspeaker array, the low-cost end-fire radiator and the structural array. In addition, the acoustic indicators used to evaluate each system are defined. Section 3 presents a comparative study of the three systems, detailing the parameters for which the simulations are run and showcasing their results.

2 Theory

2.1 Loudspeaker Array

The most straightforward way to achieve a high degree of directivity over a significant bandwidth is to use an array of multiple individual acoustic sources. As the primary concern of this paper regards only the potential directivity performance when it comes to the loudspeaker array, particular properties inherent in a loudspeaker driver are not investigated in this model. Assuming an output volume velocity U_n, where n denotes the index of the loudspeaker in the array, the total sound field radiated by N loudspeakers is equivalent to the linear superposition of the sound fields radiated by each one individually; thus, the total pressure at position r is given by

$$p\left(r\right) = \frac{j\rho_0\omega_0}{4\pi}\sum_{n=1}^{N} U_n \frac{e^{-jkr_n}}{r_n}, \tag{1}$$

where ρ_0 is the density of air, ω_0 is the angular frequency, k is the acoustic wavenumber and r_n is the distance from the n-th source to the pressure evaluation position. The complex values of the volume velocities U_n can be adjusted individually at each frequency in order to control the directivity of the system. The process for this optimisation is further elaborated in Section 2.4.

2.2 Low Cost End-Fire Acoustic Radiator

In 1991, Holland and Fahy developed a "Low-Cost End-Fire Acoustic Radiator"[13]. The design consisted of an array of holes drilled in a pipe to which a horn compression driver was attached. The resulting directivity

was shown to approach that of a multiple loudspeaker array in an end-fire configuration. The potential use of this directional sound source as an AVAS has also been investigated in [14] and [15]. Due to the simplicity of its components, the end-fire radiator may be rendered a less expensive, more robust alternative to a loudspeaker array as long as it can match its acoustic performance.

The principle of operation for the end-fire radiator is as follows: Considering a pipe where a number of holes have been drilled along its main axis, as in Figure 1, for any sound wave travelling down its length, each individual hole acts as a sound source that radiates to the external space. Given that the output from each hole is delayed due to the propagation of sound along the length of the pipe, these "sources" also display a delay between each other given by l/c_0, where l is the spacing between consecutive holes and c_0 the speed of sound in air.

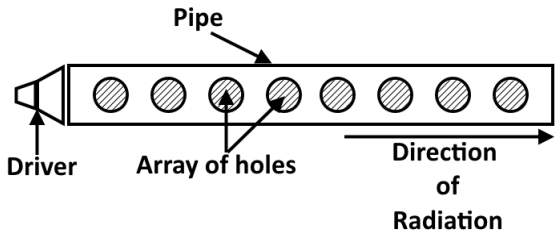

Figure 1: Example schematic, not to scale, for the end-fire radiator.

The end result is a configuration that radiates sound similarly to an end-fire array consisting of a number of sources equal to the number of holes drilled in the pipe. The directivity pattern, sensitivity and frequency range of operation of this array is primarily dependent on the physical parameters such as the size, spacing and number of the holes as well as the dimensions of the pipe itself.

Mathematical Model

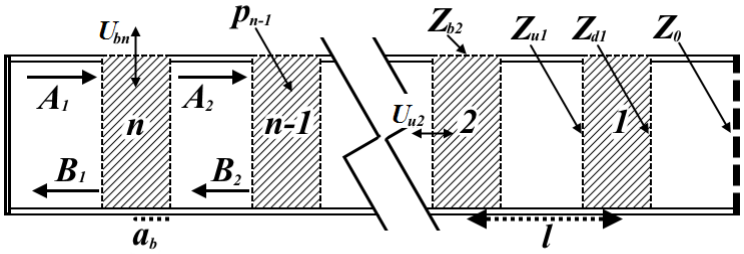

Figure 2: Schematic for the mathematical model of the end-fire radiator.

The mathematical model, which has been presented and analysed in [13] and [15], is constructed to estimate the sound field radiated by each hole and calculate the sound pressure levels in the far field. The system can be effectively modelled using acoustic transmission line theory, while approximating the fluid within the pipe as inviscid and ignoring any external coupling between holes. Figure 2 presents a schematic diagram of the end-fire radiator including the parameters considered in the mathematical model.

The impedance at the end of the pipe opposite to the source is taken as $Z_0 = \frac{\rho_0 c_0}{S}$, which corresponds to an anechoic termination, with S being the cross-sectional area of the pipe. The impedance transformation is

used to extract the impedance Z_{d1} downstream of the first hole, which is given as

$$Z_{d1} = \frac{\rho_0 c_0}{S} \left\{ \frac{Z_0 + j(\frac{\rho_0 c_0}{S} \tan(kl)}{\frac{\rho_0 c_0}{S} + iZ_0 \tan(kl)} \right\}. \tag{2}$$

It can be assumed that the acoustic pressure remains uniform in the area of the hole, given the small dimensions compared to the wavelength in question, and considering the continuity of volume velocity, the impedance upstream of the hole Z_{u1} is

$$Z_{u1} = \frac{1}{1/Z_{d1} + 1/Z_{b1}}. \tag{3}$$

In the specific case of the end-fire radiator, the impedance Z_{b1} corresponds to the value at the site of the respective hole. As the volume velocity through the hole will not generally be high enough to cause viscous flow, this radiation impedance can be approximated as

$$Z_b = \rho_0 c_0 \left[\frac{k^2}{4\pi} + j \frac{k(t + 1.5\alpha_b)}{\pi \alpha_b^2} \right], \tag{4}$$

where variables t and a_b refer to the thickness of the pipe and the diameter of each hole respectively. The value of Z_b is the same for all holes as they are identical in this system, although the sizes of the holes could be tuned to modify the response as investigated in [13], [15]. Using the value of Z_{u1} in place of Z_0 in equation (2), the downstream impedance from the second hole can be calculated, and subsequently all the respective impedances for each hole along the pipe.

In the region between the sound source and hole n, part of the plane wave of amplitude A_1 is reflected backwards with amplitude B_1, due to the impedance change caused by the hole as shown in Figure 2. The pressure p_n at the region of this hole is thus given as

$$p_n = A_1 + B_1 = 2A_1 \left(\frac{Z_{un}}{Z_{un} + \rho_0 c_0 / S} \right). \tag{5}$$

The acoustic pressure p_{n-1} at the location of each hole can then be expressed in terms of p_n, Z_{un-1}, Z_{dn} and the distance l between consecutive holes as

$$p_{n-1} = p_n \left\{ \frac{Z_{un-1} \left(\frac{\rho_0 c_0}{S} + Z_{dn} \right) [\cos(kl) - i \sin(kl)]}{Z_{dn} \left(\frac{\rho_0 c_0}{S} + Z_{un-1} \right)} \right\}. \tag{6}$$

Using equation (6), the acoustic pressure at every hole can be calculated using the known impedances. The total radiated pressure can then be calculated as in Section 2.1, using equation (1), with U_n replaced by the volume velocity through each hole of the pipe, which is given by

$$U_{bn} = \frac{p_n}{Z_{bn}}. \tag{7}$$

The mathematical model of the endfire radiator predicts a low frequency limit for its ability to achieve reasonable directivity, expressed though the relation

$$kL = 4\pi \tag{8}$$

where L is the distance between the first and last holes on the pipe. This means that the overall length of the array needs to be a least twice the wavelength of the lowest frequency.

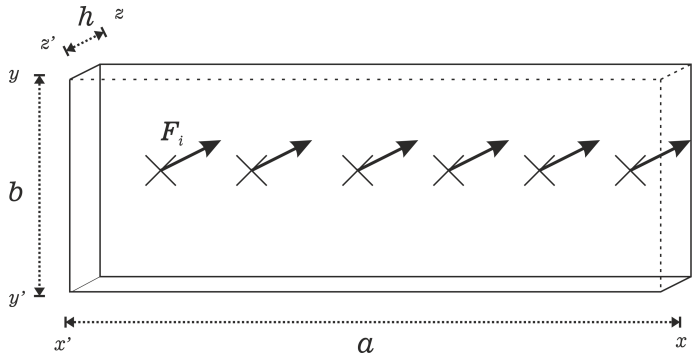

Figure 3: Schematic for the mathematical model of the structural array. A rectangular plate of thickness h is excited by a number of individual point forces F_i perpendicular to the plane defined by its sides a and b.

2.3 Structural Array

A typical dynamic loudspeaker, such as the ones used in [11] and considered when modelling the loudspeaker array in Section 2.1, utilises a voice coil to drive a diaphragm that, through its vibration, radiates the sound. This system, though capable of good performance and bandwidth, could be liable to failure when exposed to the environment when mounted on the exterior of a vehicle, and is relatively expensive to manufacture and maintain. Sound radiation could instead be achieved by an inertial actuator forcing a panel instead of a voice coil acting upon a diaphragm. This could potentially provide a lower cost with increased robustness, since the system would not rely on the relatively fragile diaphragms used in loudspeakers.

The proposed structural array would consist of a number of inertial actuators acting upon a panel which could form part of the vehicle's body to further minimise cost and better integrate the system. As with a loudspeaker array, the interference effects from vibrations caused by multiple actuators cause a directional radiated sound field. One of the key differences between the systems is that instead of multiple diaphragms being independent from each other, the vibration of the radiating panel at any one point is affected by the force applied by every actuator.

Mathematical Model

Figure 3 illustrates the geometry and approximations considered for the mathematical model of the structural array. The panel is taken as a thin rectangular plate with length a, height b and length h. The inertial actuators have been approximated by single point forces acting perpendicularly to the ab plane. In practice an actuator will have finite dimensions, however, since the actuators would be small compared to the size of the panel considered in this application, this is a reasonable approach considering the mathematical and computational simplicity that it offers.

The mathematical model for the structural array is based on the vibration of a rectangular thin plate which is simply supported along the edges, as presented in [16]. A separable solution of the transverse modal displacement for such a system is of the form

$$w_{mn}(x,y,t) = \sum_{m=1}^{\infty}\sum_{n=1}^{\infty} W_{mn} \sin k_m x \sin k_n y e^{j\omega t} \tag{9}$$

where W_{mn} is the modal amplitude and m, n are the modal indices for modes along the x and y axes respectively. For boundary conditions of zero transverse displacement along the edges, the wavenumber eigenvalues in each coordinate direction are

$$\begin{aligned} k_m &= m\pi/a, \qquad m = 1,2,3,... \\ k_n &= n\pi/b, \qquad n = 1,2,3,... \end{aligned} \tag{10}$$

and the discrete frequencies at which the system resonates are given by

$$\omega_{mn} = \left(\frac{EI}{\rho h}\right)^{1/2} \left[k_m^2 + k_n^2\right], \tag{11}$$

where E is Young's modulus of elasticity and ρ is the density of the plate, while I is the moment of inertia per unit width. For an input forcing function of a point force, $f(x,t) = F\delta(x - x_i)\delta(y - y_i)e^{j\omega t}$ located at x_i, y_i, the modal amplitudes are given by

$$W_{mn} = \frac{4F \sin k_m x_i \sin k_n y_i}{M(\omega^2 - \omega_{mn}^2)}, \tag{12}$$

where M is the mass of the plate.

The acoustic pressure in the far field, at a distance r from the defined centre point of the plate can be calculated using the Rayleigh integral in terms of the complex transverse velocities $\dot{w}(\boldsymbol{r}_S)$ at points $\boldsymbol{r}_S$ on the surface S, such that the pressure is given by

$$p\left(\boldsymbol{r}\right) = \int_S \frac{j\omega\rho_0 \dot{w}(\boldsymbol{r}_s)e^{-jkR}}{2\pi R} dS, \tag{13}$$

where $R = |\boldsymbol{r} - \boldsymbol{r}_s|$. The complex velocity $\dot{w}(\boldsymbol{r}_S)$ can be expressed as

$$\dot{w}(\boldsymbol{r}_S) = \dot{W}_{mn} \sin\left(\frac{m\pi x}{a}\right)\left(\frac{n\pi y}{b}\right) \qquad \{^{0\leq x\leq a}_{0\leq y\leq b}\}. \tag{14}$$

The total acoustic pressure at a point described by the coordinates (r, θ, ϕ) in the far field, radiated from the panel upon which a number of N point forces act at coordinates (x_i, y_i), is expressed upon evaluation of the integral in equation (13) as

$$p\left(r,\theta,\phi\right) = \sum_{m=1}^{\infty}\sum_{n=1}^{\infty} \frac{j\omega\rho_0 e^{-jkr}}{2\pi r} \frac{ab}{mn\pi^2} \left[\frac{(-1)^m e^{-j\alpha} - 1}{(\alpha/m\pi)^2 - 1}\right]\left[\frac{(-1)^n e^{-j\beta} - 1}{(\beta/n\pi)^2 - 1}\right] \sum_{i=1}^{N} \dot{W}_{mn}(i), \tag{15}$$

where $\alpha = ka\sin\theta\cos\phi$ and $\beta = kb\sin\theta\sin\phi$.

2.4 Array Optimisation and Performance Metrics

A method of quantifying a system's directivity performance is through the acoustic contrast between the average mean square pressure in a bright zone and the average mean square pressure in a dark zone. As defined in [17], the acoustic contrast at a given frequency is

$$AC = \frac{\boldsymbol{p}_B^H \boldsymbol{p}_B}{\boldsymbol{p}_D^H \boldsymbol{p}_D} = \frac{\boldsymbol{q}^H \boldsymbol{H}_B^H \boldsymbol{H}_B \boldsymbol{q}}{\boldsymbol{q}^H \boldsymbol{H}_D^H \boldsymbol{H}_D \boldsymbol{q}}, \tag{16}$$

where $\boldsymbol{q}$ is the vector containing the complex source strengths, $\boldsymbol{p}_B$, $\boldsymbol{p}_D$ are the vectors containing the amplitudes of the complex pressures in the bright and dark zones respectively, $\boldsymbol{H}_B$, $\boldsymbol{H}_D$ are the matrices of complex transfer responses between the sources and the measuring points in the bright and dark zones, while the superscript H indicates the Hermitian complex conjugate transpose.

Source Strength Optimisation

The definition of two distinct zones between which a contrast can be measured allows for the formulation of an optimisation problem. The value of acoustic contrast is maximised when $\boldsymbol{p}_B^H \boldsymbol{p}_B$ is maximised under the constraint that $\boldsymbol{p}_D^H \boldsymbol{p}_D$ remains constant at value d, resulting in the *Lagrangian*:

$$L = \boldsymbol{q}^H \boldsymbol{H}_B^H \boldsymbol{H}_B \boldsymbol{q} - \lambda(\boldsymbol{q}^H \boldsymbol{H}_D^H \boldsymbol{H}_D \boldsymbol{q} - d) \tag{17}$$

	Loudspeaker Array
No. of loudspeakers	6
Spacing between loudspeakers	14.3 cm
Array length	71.5 cm
	End-Fire Radiator
No. of holes	10
Hole radius	6 mm
Spacing between holes	8 cm
Effective array length	72 cm
Pipe length	80 cm
Pipe radius	2 cm
Pipe thickness	3 mm
	Structural Array
No. of actuators	6
Spacing between actuators	14.3 cm
No. of modes considered (x-direction)	12
No. of modes considered (y-direction)	8
Panel dimensions	1 m $\times$ 0.2 m $\times$ 3 mm
Panel density	2700 kg/m^3
Young's modulus	70 GPa
Poisson ratio	0.334
Frequency of first mode	192.25 Hz

Table 1: Set simulation parameters specific to each system.

with the positive and real Lagrange multiplier λ. By setting the complex differential of L with respect to $\boldsymbol{q}$ to zero, and under the assumption that $\boldsymbol{H}_D^H \boldsymbol{H}_D$ is invertible, yields the eigenvalue problem

$$\lambda \boldsymbol{q} = [\boldsymbol{H}_D^H \boldsymbol{H}_D]^{-1} \boldsymbol{H}_B^H \boldsymbol{H}_B \boldsymbol{q} = \boldsymbol{M} \boldsymbol{q}. \tag{18}$$

The source strength vector $\boldsymbol{q}$ that maximises the acoustic contrast is proportional to the eigenvector of the matrix $\boldsymbol{M}$ corresponding to its largest eigenvalue [17]. Therefore by adjusting the source strengths according to the values of said eigenvector, the overall radiated sound field will be characterised by the maximum possible acoustic contrast. In the cases of the loudspeaker array and the structural array, this would be the method of achieving the highest degree of directivity, by controlling each individual loudspeaker driver or actuator respectively.

3 Simulations

3.1 Simulation Parameters

The performance of the investigated systems has been evaluated through simulations using the mathematical models presented above. Vehicle warning sounds currently in use and in development are mostly limited to frequencies between 100 Hz and 3 kHz. An operating range from 40 Hz to 4 kHz is therefore deemed as suitable to include all potential components of a warning sound and provide a clear picture of each system's frequency response.

The complex acoustic pressure is estimated using equations (1) and (15) for a distance $r = 5\ m$ from the centre of each array and a θ angle coverage of 360^o, with the ϕ angle kept at 0^o, corresponding to the plane of movement for the vehicle. Calculations are performed for 360 measurement points evenly distributed along

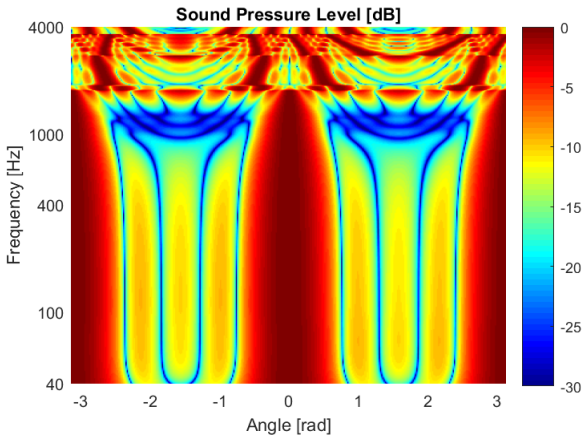

(a) Loudspeaker Array

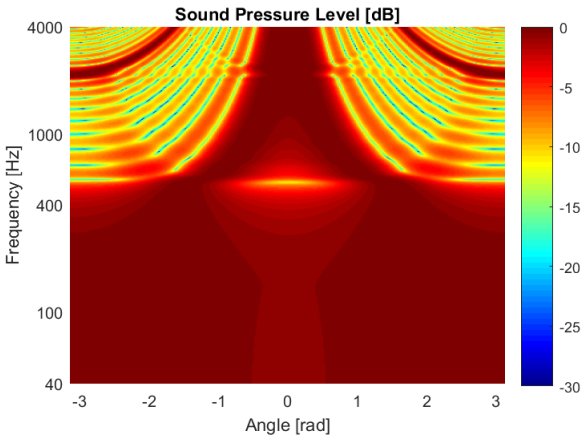

(b) End-Fire Radiator

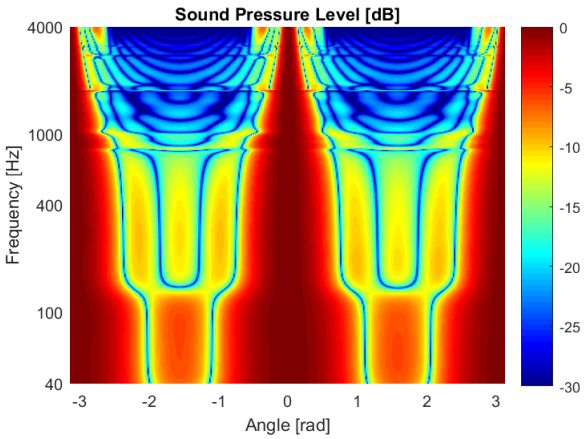

(c) Structural Array

Figure 4: Normalised SPL frequency response as a function of the observation angle for a simulated six loudspeaker array, the end-fire radiator, and the structural array.

a 5 m radius circle sharing the centre of the array in question. A designated bright zone covering an angle $\theta_B = 60^o$ in the forward direction, and the dark zone defined by its explementary angle θ_D, are used to calculate the acoustic contrast and optimise the outputs of the loudspeaker and structural arrays to achieve the highest possible degree of directivity. Other general parameters which are common in all simulations are the density of air taken as $\rho_0 = 1.225\ kg/m^3$, and the speed of sound in air as $c_0 = 340.27\ m/s$.

Table 1 shows the parameters which are associated with each system. Six loudspeakers form the loudspeaker array, as with the array used for the system presented in [11]. Investigations of the effects that the physical characteristics have on the directivity performance have been carried out in [13] and [15]. The physical characteristics of the pipe are chosen to ensure the optimum compromise between operational bandwidth at the frequencies needed for warning sounds and implementation within the confines of a passenger vehicle. The structural array features six actuators, placed at intervals identical to the loudspeakers in the above case, to offer a more direct and substantial comparison between their performances. The panel, placed with its main plane facing the forward direction, has been given the dimensions of $1 \times 0.2 \times 0.003\ m$, a reasonable size to fit in a vehicle, and its material chosen has been chosen as aluminium.

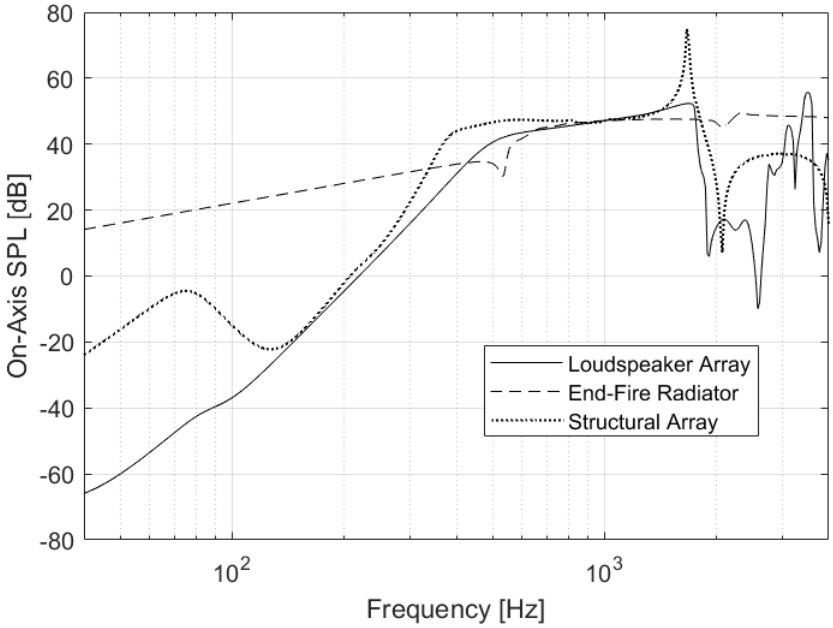

Figure 5: On-axis SPL frequency response for a six loudspeaker array, the end-fire radiator and the structural array.

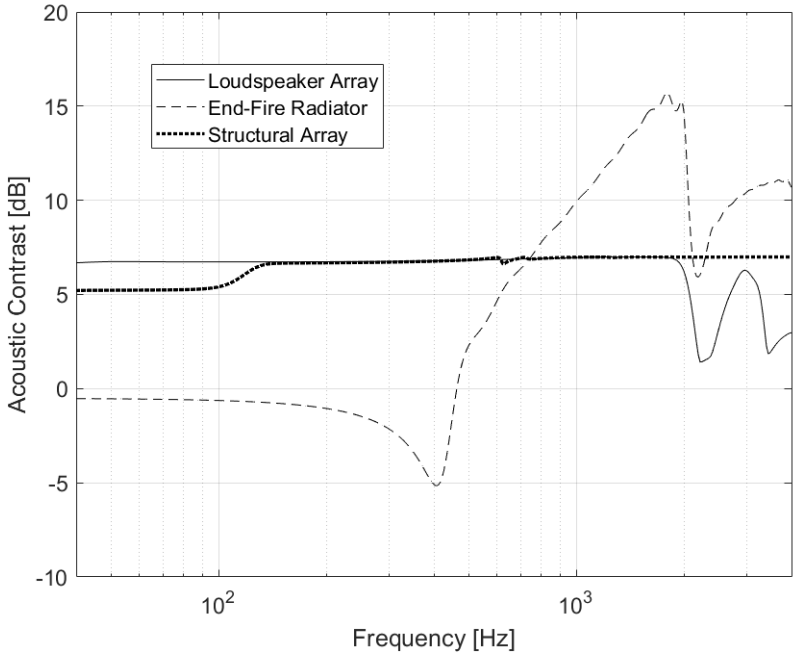

Figure 6: Acoustic contrast frequency response comparison between a six loudspeaker array, the end-fire radiator and the structural array.

3.2 Comparison of Results

Figure 4 shows the Sound Pressure Level (SPL) frequency response as a function of the observation angle for the three simulated systems. The values have been normalised to allow a more straightforward comparison of the systems' directivity. The zero degree angle corresponds in each case to the presumed forward direction; both the loudspeaker array and the structural array have been optimised to maximise their output within the aforementioned θ_B angle centred around this direction.

Given the parameters set in Table 1, the low frequency limit of the endfire radiator estimated according to equation 8 should be as high as 945 Hz. Still, an observable albeit reduced directivity remains for frequencies above 500 Hz. Its directivity performance improves as frequency increases until the 2 kHz mark, however beyond that side lobes of significant intensity appear. The loudspeaker array maintains its directivity across the entire spectrum investigated, although along with the increase in frequency, there is an overall increase in the output SPL in every direction. The structural array also displays a directional behaviour throughout the tested frequency range, while limiting the increase in SPL observed in the previous case.

The on-axis SPL frequency response for each configuration is shown in Figure 5. In this instance no normalisation has been performed, but for better comparison the gain has been adjusted so that the estimated SPL at 1kHz is equal for all three cases. The low frequency limit of the endfire radiator seen in Figure 4 is also visible here. In the case of the loudspeaker and structural arrays, the response across the investigated frequency range is characterised by a similar low frequency limit as well as dips and peaks at frequencies above 1.5 kHz, behaviour which is not evident when investigating the normalised output.

Acoustic Contrast

Figure 6 shows the acoustic contrast over frequency for all three systems. Although the end-fire radiator appears capable of achieving the highest contrast, its operational bandwidth is limited and its performance at frequencies below 1 kHz is rather poor. Both the loudspeaker and structural arrays show a flat response across the majority of the frequency range investigated, indicating a large operational bandwidth, although the maximum contrast achieved is significantly lower than that of the end-fire radiator. While the structural array displays a low frequency limit, presumably due to the dominance of the first mode of the plate, its performance at frequencies higher than 2 kHz surpasses that of the loudspeaker array.

4 Conclusions

This paper presents two directional sound system concepts for the implementation of warning systems in an electric vehicle, in the form of an end-fire radiator and a structural actuator array. Cost efficiency and durability given the application were taken into account for these designs. Analytical mathematical models were developed for both systems which allow for a parameter optimisation, given the restrictions imposed by their in-vehicle implementation, to produce directional sound fields across a frequency range suitable for warning sounds. The analytical models were used to perform a series of simulations to compare the performance of the systems to a conventional loudspeaker array. Simulation results indicate that all systems are capable of achieving high directivity, however in the case of the end-fire radiator the operational bandwidth is limited. The structural array displays a constant acoustic contrast over frequency and surpasses the performance of the loudspeaker array at the upper end of the investigated frequency range.

Acknowledgements

The authors gratefully acknowledge the European Commission for its support of the Marie Sklodowska Curie program through the ETN PBNv2 project (GA 721615).

References

[1] N. Campello-Vincente et al., *The Effect of Electric Vehicles on Urban Noise Maps*, Applied Acoustics, Vol. 116, No. 7/8, January 2017, pp. 59-64.

[2] N. Campillo-Davo, A. Rassili, *NVH Analysis Techniques for Design and Optimisation of Hybrid and Electric Vehicles*, Shaker Verlag Publications (2016).

[3] G. Marberg, *Noise from Electric Vehicles - A Literature Survey*, Compett (2013).

[4] M. Muirhead, L.K. Walter, *Analysis of STATS19 Data to Examine the Relationship Between the Rate of Vehicle Accidents Involving Pedestrians and Type Approval Noise Levels*, Transport Research Laboratory, July 2011.

[5] J. Wu, R. Austin, C.L. Chen, *Incidence Rates of Pedestrian and Bicyclist Crashes by Hybrid Electric Passenger Vehicles: An Update*, NHTSA, US Department of Transportation, October 2011.

[6] U. Sandberg, L. Goubert, P. Mioduszewski, *Are Vehicles Driven in Electric Mode So Quiet That They Need Acoustic Warning Signals?*, in M. Burgess, editor, *Proceedings of The 20th International Congress on Acoustics, Sydney, Australia, 2010 August 23-27*, Sydney (2010), pp. 1835-1845.

[7] National Highway Traffic Safety Administration (NHTSA), *Minimum Sound Requirements for Hybrid and Electric Vehicles - Final Rule*, US Department of Transportation, November 2016.

[8] Economic Commission for Europe of the United Nations (UNECE), *Regulation No 138 of the Economic Commission for Europe of the United Nations (UNECE) Uniform provisions concerning the approval of Quiet Road Transport Vehicles with regard to their reduced audibility [2017/71]*, January 2017.

[9] Japan Automobile Standards Internationalisation Centre (JASIC), *Guidelines for Measures Against Quietness Problem of Hybrid Vehicles*, Informal Group on Quiet Road Transport Vehicles, January 2010.

[10] F. Dubois, G. Baudet, J.C. Chamard, *EVADER: Electric Vehicle Alert for Detection and Emergency Response* , in *Proceedings of the Acoustics 2012 Nantes Conference, 2012 April 23-27*, Nantes (2012), pp.1051-1055.

[11] D. Quinn, J. Mitchell, P. Clark, *Development of a next-generation audible pedestrian alert system for EVs having minimal impact on environmental noise levels - project eVADER* , in *Proceedings of 43rd International Congress on Noise Control Engineering, Melbourne, Australia, 2014 November 16-19*, Melbourne (2014).

[12] E. Parizet, W. Ellermeier, R. Robart, *Auditory Warnings for Electric Vehicles: Detectability in Normal-Vision and Visually-Impaired Listeners*, Applied Acoustics, Vol. 86, December 2014 pp. 50-58.

[13] K.R. Holland, F.J. Fahy, *A Low-Cost End-Fire Acoustic Radiator*, Journal of the Audio Engineering Society, Vol. 39, No. 7/8, July/August 1991, pp. 540-550.

[14] J. Cheer, T. Birchall, P. Clark, J. Moran, S.J. Elliott, F.M. Fazi, *Design and implementation of a directive electric car warning sound*, Proceedings of the Institute of Acoustics, Vol. 35, Pt. 1 (2013).

[15] J. Carbajo, S.J. Elliott, J. Cheer, *Study of a low-cost end-fire array for use in electric vehicles*, in W. Kropp, editor, *Proceedings of The 2016 International Congress and Exhibition on Noise Control Engineering, Hamburg, Germany, 2016 August 21-24*, Hamburg (2016), pp. 4456-4466.

[16] C.R. Fuller, S.J. Elliott, P.A. Nelson, *Active Control of Vibration*, Academic Press, London (1996).

[17] S.J. Elliott, J. Cheer, *Regularisation and Robustness of Personal Audio Systems*, ISVR Technical Memorandum, No. 995, December 2011.